Cement and Concrete Research 41 (2011) 113–122

Contents lists available at ScienceDirect

Cement and Concrete Research

journal homepage: http://ees.elsevier.com/CEMCON/default.asp

The origin of the pozzolanic activity of calcined clay minerals: A comparison between kaolinite, illite and montmorillonite

Rodrigo Fernandez [b,*], Fernando Martirena [a], Karen L. Scrivener [b]

[a] Centro de Investigación y Desarrollo de Estructuras y Materiales (CIDEM), Universidad Central "Marta Abreu" de Las Villas, 54830 Santa Clara, Cuba
[b] Laboratory of Construction Materials, IMX, Ecole Polytechnique Fédérale de Lausanne, 1015 Lausanne, Switzerland

ARTICLE INFO

Article history:
Received 12 May 2010
Accepted 24 September 2010

Keywords:
Metakaolin
Pozzolan
Calcined clay minerals
Amorphous material
Microstructure

ABSTRACT

This paper investigates the decomposition of three clayey structures (kaolinite, illite and montmorillonite) when thermally treated at 600 °C and 800 °C and the effect of this treatment on their pozzolanic activity in cementitious materials. Raw and calcined clay minerals were characterized by the XRF, XRD, ^{27}Al NMR, DTG and BET techniques. Cement pastes and mortars were produced with a 30% substitution by calcined clay minerals. The pozzolanic activity and the degree of hydration of the clinker component were monitored on pastes using DTG and BSE-IA, respectively. Compressive strength and sorptivity properties were assessed on standard mortars. It was shown that kaolinite, due to the amount and location of OH groups in its structure, has a different decomposition process than illite or montmorillonite, which results in an important loss of crystallinity. This explains its enhanced pozzolanic activity compared to other calcined clay–cement blends.

1. Introduction

Calcined kaolinite, or metakaolin, has been well studied in recent years and has proven to have very good pozzolanic properties [1,2]. Its potentially beneficial use in concrete has been well established; for example, it has been shown that the replacement of cement by 5%–10% of metakaolin can drastically improve the mechanical properties of concrete, as well as its durability [3,4]. However, the origin of the pozzolanic properties of calcined kaolinites, in contrast to other clay minerals, is not well understood.

Crystallography has helped a lot in understanding the effects of thermal treatment on the structure of clay minerals. Brindley [5] laid the groundwork in this field by investigating the kaolinite–mullite reaction series back in 1959. He used ^{27}Al NMR to suggest a semi-crystalline structure for metakaolin. Around 30 years later, Mackenzie [6] proposed a revised structure including only 4- and 6-coordinated Al, but Rocha and Klinowski [7] confirmed the occurrence of 5-coordinated aluminium in the structure based on previous work on aluminosilicates [8,9]. Although much of the interest with NMR has been focused on kaolinite transformations, some papers also report some findings on the thermal behaviour of illite [10] and montmorillonite [11].

In parallel, research in cement and concrete has looked at the pozzolanic properties of various calcined clay minerals by mixing them with lime or cement [i.e. 12,13]. It was concluded that kaolinite was the most reactive type of clay. Many of these works also looked at the influence of calcinations parameters such as time and temperature on the final properties of the blends, aiming at optimizing the pozzolanic reactivity of metakaolin for potential industrial applications [14,15]. However, little effort has been put into linking the pozzolanic reactivity of calcined clay minerals to the decomposition process.

This paper investigates three types of clay minerals commonly found in the earth's crust: kaolinite, illite and montmorillonite. The aim is to compare the decomposition mechanisms of these structures and see how they influence the pozzolanic properties of the materials when mixed with cement. The work includes the characterization of the clay structures before and after calcination, a study of the pozzolanic activity of calcined clay minerals–cement blends and the assessment of the mechanical and sorptivity properties on mortars.

2. Materials and methods

Kaolinite, illite and montmorillonite, referred to as standards clay minerals, were purchased from Ward's Natural Science [16] and were used as received. These clay minerals are natural materials that cannot be considered pure minerals as they contain some impurities such as quartz, feldspars or other clay types in minor amounts. Their structure and ideal formulas are presented in Fig. 1. Aluminosilicate minerals are formed by the stacking of layers composed of alternating tetrahedral and octahedral sheets [17]. In the case of kaolinite, because its layer is formed of two sheets only, two distinct interlayer surfaces coexist: one with aluminate groups and one with silicate groups. The adjacent layers are linked by hydrogen bonding involving aluminol (Al–OH) and siloxane (Si–O) groups. These bonding forces mean kaolin is a nonswelling clay [18]. Also, in the plane of atoms

* Corresponding author. Tel.: +41 21 693 28 43; fax: +41 21 693 58 00.
E-mail address: fernandezrod@gmail.com (R. Fernandez).

0008-8846/$ – see front matter © 2010 Published by Elsevier Ltd.
doi:10.1016/j.cemconres.2010.09.013

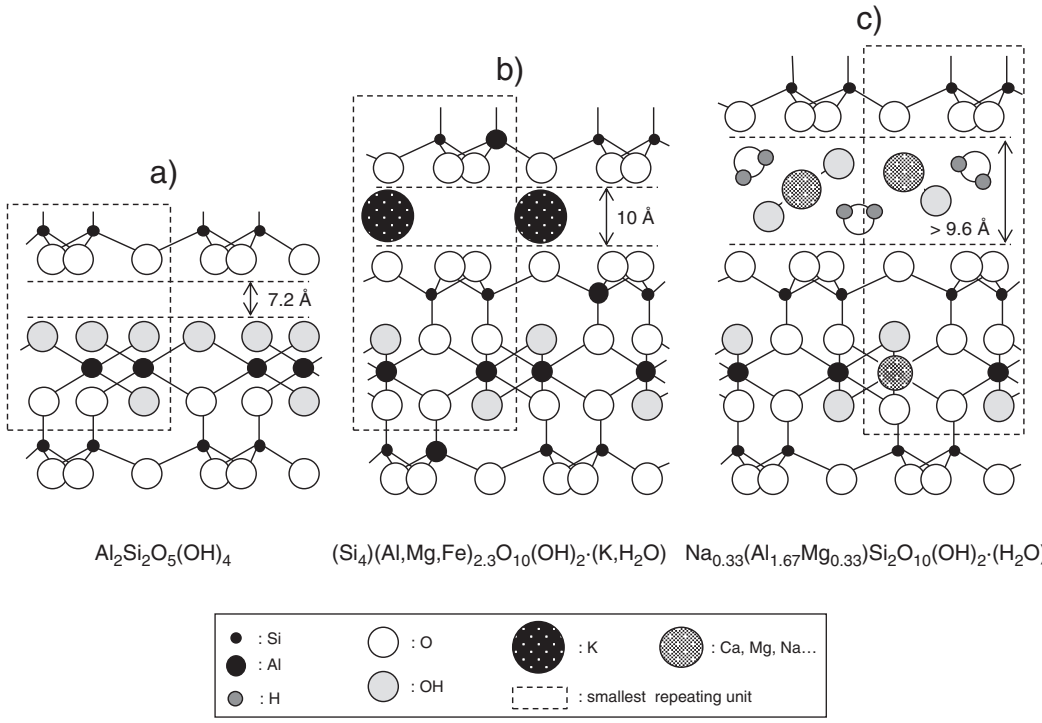

Fig. 1. Structures and ideal formulas of kaolinite (a), illite (b) and montmorillonite (c) (adapted from Grim [19])[1].

common to both sheets, two-thirds of the atoms is oxygen, and one third is hydroxyls. In the two other clayey structures studied, the unit layer is formed by an octahedral sheet of alumina trapped between two sheets of silicon tetrahedrons. Therefore, the adjacent interlayer surfaces are similar and composed of siloxane groups only. The nature of the interlayer bond differs from the kaolinite case. For illite, because about one-fourth of the silicon positions are filled by aluminium, the resulting charge deficiency of 1.3–1.5 per unit cell is balanced by potassium between the layers forming a strong bond. Montmorillonite has a crystal structure similar to illite, except that isomorphous substitution usually occurs in the octahedral sheet, where every sixth aluminium is replaced by magnesium. The resulting balance charge between successive layers is made by different cations such as sodium or calcium forming adsorption complexes with water molecules. These bonds are weak and easily separated by cleavage or adsorption of other polar liquids. As a result, the position and amount of hydroxyl groups differ significantly from one structure to another. For kaolinite, the majority of hydroxyl groups are located on the interlayer surface of the octahedral sheet. For illite and montmorillonite, apart from the hydroxyl groups that could be present at the particle broken edges, most of the hydroxyl groups are located in the core of a layer, between two tetrahedral sheets.

Standard clay minerals and other raw materials were characterised by X-ray fluorescence using a Bruker AXS S4 Explorer spectrophotometer operating at a power of 1 kW and equipped with a Rh X-ray source. Results can be seen in Table 1.

X-Ray diffraction patterns for untreated and calcined materials were recorded on a Panalytical X'Pert Pro MPD diffractometer in a θ–θ configuration employing CuKα radiation (λ = 1.54 Å) with a fixed divergence slit size of 0.5° and a rotating sample stage. The samples were scanned between 4 and 70° 2θ with the X'Celerator detector. The step size and time per step were set to 0.017° 2θ and 80 s, respectively. Diffraction patterns of the raw materials are shown in Fig. 2. Peaks appearing at low angles correspond to the diffraction of the basal planes of the clay structures. They are located at 12.3, 9 and 7° 2θ for kaolinite, illite and montmorillonite, respectively. The presence of companion minerals such as albite, cristobalite and quartz could be detected with this technique, indicating that these materials are not pure.

The ^{27}Al NMR experiments were performed on a Bruker ASX 500 spectrometer, in a 11.7 Tesla field, operating at 129.80 MHz for ^{27}Al. Spectra were recorded at a 10-kHz spinning rate in 4-mm ZrO_2 rotors. All experiments employed single pulse (pi/12) excitation width pulse of 0.5-ms pulse time without ^{1}H decoupling and a 1-s relaxation delay. A Mettler–Toledo TGA/SDTA 851 instrument was used for thermogravimetric measurements, with a heating rate of 10 °C/min from 30 °C to 900 °C. A 30-ml/min nitrogen flux was used in the heating chamber in order to avoid carbonation of the samples during the experiment. The tangent method was used to measure water loss for the dehydroxylation of the clay minerals and for the decomposition of the calcium hydroxide in the pastes. The amount of calcium hydroxide was calculated from the weight loss in the 450–600 °C range and was expressed relative to the ignited weight of cement in the mix, as suggested by Marsh [20]. Particle size distributions were measured with a Malvern Mastersizer type S laser beam granulometer, allowing measurements of particles sizes ranging from 0.05 μm to 900 μm in dispersion. Cement pastes were dispersed in isopropanol, whereas clay minerals were dispersed in a 0.01% PAA solution (poly acrylic acid). A Micromeritics Accupyc 1330 V2 instrument was used for bulk density measurements, and a Micromeritics Gemini 2375 V4 instrument allowed the determination of a specific surface (BET). The standard clay minerals were calcined at 600 and 800 °C in a laboratory furnace. 50 g of clay was put into cylindrical alumina crucibles, which were introduced in the furnace prior to heating. The heating rate was 300 °C/h and the time at peak temperature was 60 min. Cooling was done rapidly by removing the crucibles from the hot furnace and spreading the material on a metal plate.

For the study on pastes and mortars, a CEM I 52.5R cement was used. A filler, consisting of finely ground quartz, was also used for

[1] All formulas are reduced to the smallest unit formula; they do not reflect unit cell composition. Many variations can occur, particularly in the interlayer positions of the montmorillonite. Cations such as Ca^{++} and Na^{+} are often present.

Table 1
Chemical analysis of standard clay minerals, filler and cement.

% Weight	SiO_2	Al_2O_3	Fe_2O_3	CaO	MgO	SO_3	K_2O	MnO	Na_2O	Others	LOI	Total	Alkalies % (Na_2Oeq)
Kaolinite	48.00	36.40	0.85	0.14	0.11	0.03	0.48	0.01	0.02	0.00	13.41	99.44	0.33
Illite	58.68	19.25	5.04	1.29	2.50	0.17	6.12	0.05	0.19	0.00	5.71	99.00	4.22
Montm.	63.15	20.09	3.96	1.15	2.27	0.51	0.54	0.02	2.22	0.00	5.90	99.81	2.57
Filler	99.54	-	-	0.02	0.02	0.00	0.01	0.00	-	0.00	-	99.59	0.01
Cem I 52.5R	21.03	5.01	2.54	63.45	2.05	3.01	1.02	0.04	0.26	0.24	1.34	100.00	0.93

comparison with the pozzolans by assuming it would behave as an inert material and would not react with calcium hydroxide. It was used to substitute cement at the same level of the calcined clay minerals. The mix designs are presented in Table 2. For the study, 30 °C was chosen as the reference temperature to better simulate tropical climates and accelerate reaction, and 30% was chosen as the reference substitution level. The pastes were studied by XRD, TGA, and NMR. Mortars were prepared following European Standards (EN) 196-1 for the assessment of compressive strength. Sorptivity and capillary porosity were also measured following the Swiss standard SIA 262/1. Scanning electron microscopy was used in the back-scattered electron (BSE) mode on polished sections for automated image analysis on both pastes and mortars. It allowed the determination of the degree of hydration of the clinker component at 28 days by gray level differentiation [21]. For each sample, 120 images were taken, with a magnification of 1500×. The same mode was used with a magnification of 800× for a qualitative analysis on few images.

3. Results and discussion

3.1. Effect of calcinations on standard structures

The DTG curves for the standard clay minerals are presented in Fig. 3. The small mass loss in the range of 30–200 °C for kaolinite and illite can be assigned to the drying of the absorbed water. Montmorillonite exhibits a more significant release of water from between the layers. The removal of the OH groups (dehydroxylation) can be observed in the range 400–800 °C. The position of the dehydroxylation peak depends mainly on the type of structure and the binding of the hydroxyls, whereas its shape and range depend more on the crystallinity or particle size distribution [22]. The size of the peak is indicative of the amount of hydroxyls originally present in the structure; as seen in Fig. 1, kaolinite incorporates more OH groups than the other clay minerals. However, the tested materials are not pure with different proportions of companion minerals such as quartz and other clay structures. Therefore, comparisons based on this technique could only be misleading as mass losses are normalized by the sample mass.

Curves for the calcined products are included in the graphs in order to show how effective a given thermal treatment has been on the clay dehydroxylation. For kaolinite, dehydroxylation can be considered to be complete at 600 °C, as the amount of hydroxyls remaining in the sample after such thermal treatment is negligible. The curve for illite at 600 °C shows that not all hydroxyls have been removed, suggesting that the structure is not completely decomposed. As for montmorillonite, the fact that the size of the peak is maintained after a 600 °C treatment indicates that most of the dehydroxylation occurs between 600 °C and 800 °C.

Fig. 4 shows the XRD patterns for the standard clay minerals and their calcined products. At 600 °C, practically all peaks corresponding to kaolinite have disappeared, indicating a very significant loss of crystallinity. Calcination at 800 °C does not produce many additional changes to the decomposed structure. Traces of muscovite and some quartz could be identified, whose structures have not been altered by temperature. XRD patterns of illite calcined at both 600 °C and 800 °C show little change from the original material. It is interesting to note that dehydroxylation observed by DTG has almost no effect on the crystallinity observed by XRD for this phase, where only a small drop

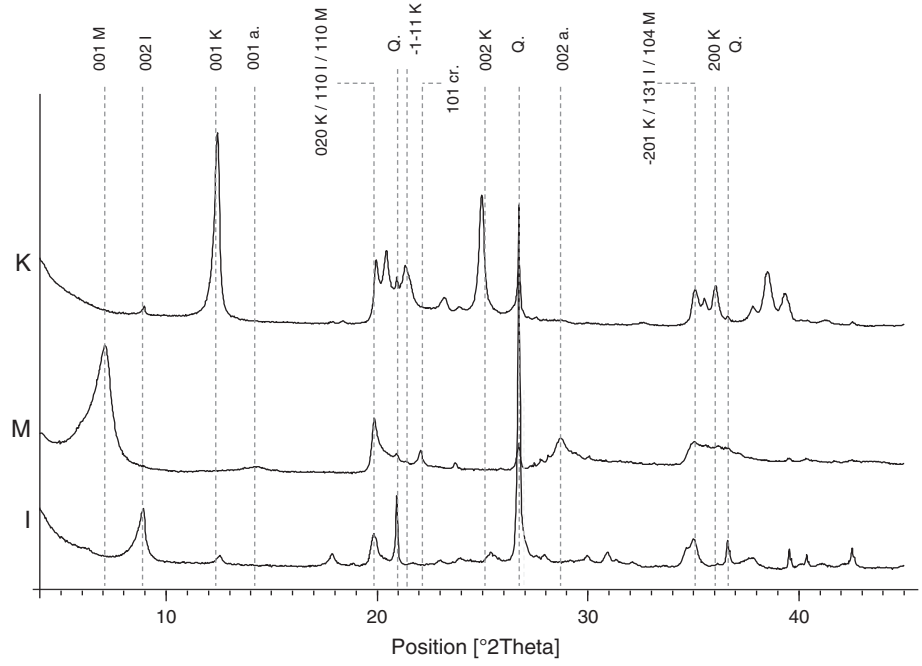

Fig. 2. X-ray diffraction of standard clay minerals (K: kaolinite, M: montmorillonite, I: illite, a.: albite, cr.: cristobalite, and Q: quartz).

Table 2
Series of pastes and mortars.

Label for Pastes/Mortars	Type of Substituent	Activation Temperature	% Substituent	% OPC	w/b for Pastes/ Mortars
k600/K600	Kaolinite	600 °C	30%	70%	0.4/0.5
k800/K800		800 °C	30%	70%	0.4/0.5
i600/I600	Illite	600 °C	30%	70%	0.4/0.5
i800/I800		800 °C	30%	70%	0.4/0.5
m600/M600	Montmorillonite	600 °C	30%	70%	0.4/0.5
m800/M800		800 °C	30%	70%	0.4/0.5
Filler/Filler	Filler	–	30%	70%	0.4/0.5
opc/OPC	–	–	0%	100%	0.4/0.5

in intensity could be seen for the basal planes (002, 004, 006, and 0010). For montmorillonite, the collapse of the basal planes with temperature is apparent as the 001 plane shifts from 12.3 Å to 9.6 Å. This is due to the removal of the interlayer water originally contained in the sample and so is unlikely to contribute to the activation of the materials from a pozzolanic perspective. This decomposition cannot be compared to the kaolinite decomposition as some peaks remain after the thermal treatments. The presence of rather inert companion minerals such as albite (a feldspar) and muscovite are useful indicators of montmorillonite decomposition, as their relative signal increases with temperature, indicating that their contribution to the total amount of crystalline material increases.

The effect of dehydroxylation on the different clayey structures was also studied by ^{27}Al NMR, as shown in Fig. 5, where the different coordination sites of Al can be distinguished. The sharp peak observed around 1 ppm for the reference kaolinite has been previously attributed to Al$^{[VI]}$ [e.g., 6,23]. In this case, the sharpness of this peak indicates a well ordered octahedral structure. After calcination at 600 °C, two peaks appear, at 28 ppm and 56 ppm, attributed to Al$^{[V]}$ and Al$^{[IV]}$, respectively [7–9]. It is interesting to note that the Al$^{[V]}$ peak increases with increasing temperature to be the dominant site for Al at 800 °C. This clearly indicates a breakdown in order of the original crystalline structure. Surprisingly, these substantial changes occurring in the surroundings of the aluminium, between 600 °C and 800 °C, as revealed by NMR, are not indicated by the change in XRD and DTG patterns, which show only small changes. This suggests that dehydroxylation alone does not explain the disordered state for metakaolinite and there must be another process that increases the number of 5-coordinated Al when going from 600 °C to 800 °C. Following Rocha [7], this could be the modification of the short-range

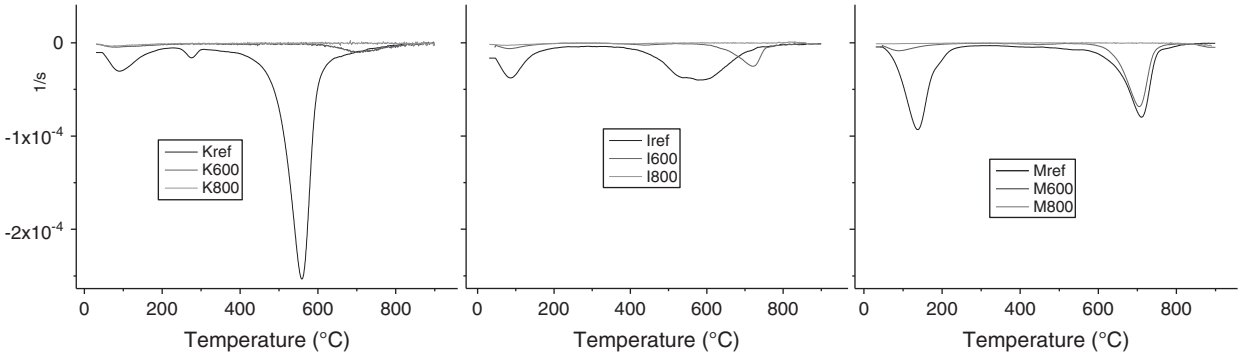

Fig. 3. DTG curves of standard clay minerals and their calcined products.

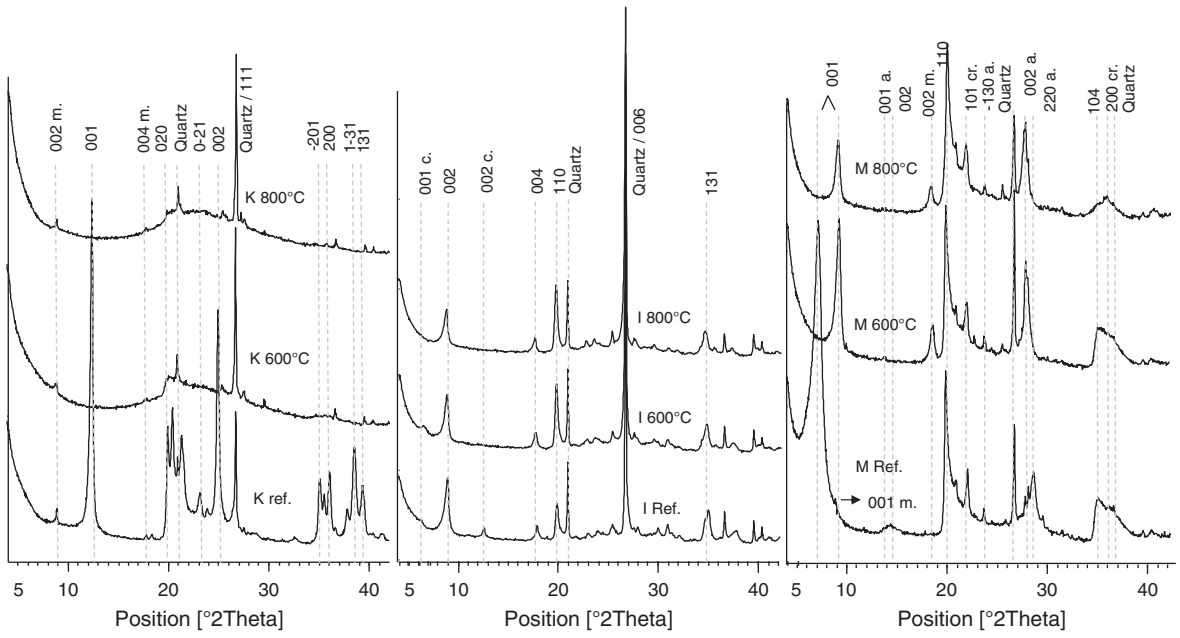

Fig. 4. X-ray patterns of standard clay minerals and their calcined products (K: kaolinite, I: illite, M: montmorillonite, m: muscovite, c: clinochlore, and cr: cristobalite).

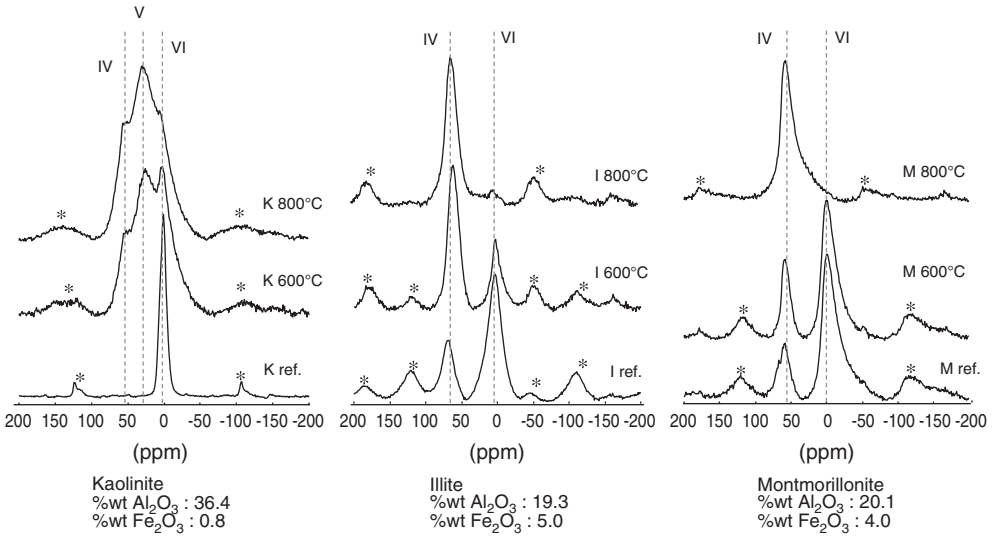

Fig. 5. ^{27}Al NMR spectra of standard clay minerals and their calcined products.

order of Si in metakaolinite, whose ^{29}Si NMR studies indicated that a range of Qm(nAl) environments are formed with Al in all three coordination states (IV, V, and VI). This hypothesis could also explain the persistence of the 6-coordinated Al at 800 °C, which was rather unexpected due to the complete dehydroxylation observed by DTG for this temperature.

The ^{27}Al NMR spectra for illite and montmorillonite exhibit 2 peaks with maxima at 1 ppm and 56 ppm, which can be assigned to $Al^{[VI]}$ and $Al^{[IV]}$, respectively. The shape and position of the peaks correspond well with previously published studies on these types of clay [10,11]. The presence of the 4-coordinated peak indicates that Al is substituting Si in tetrahedral positions, which is very common in

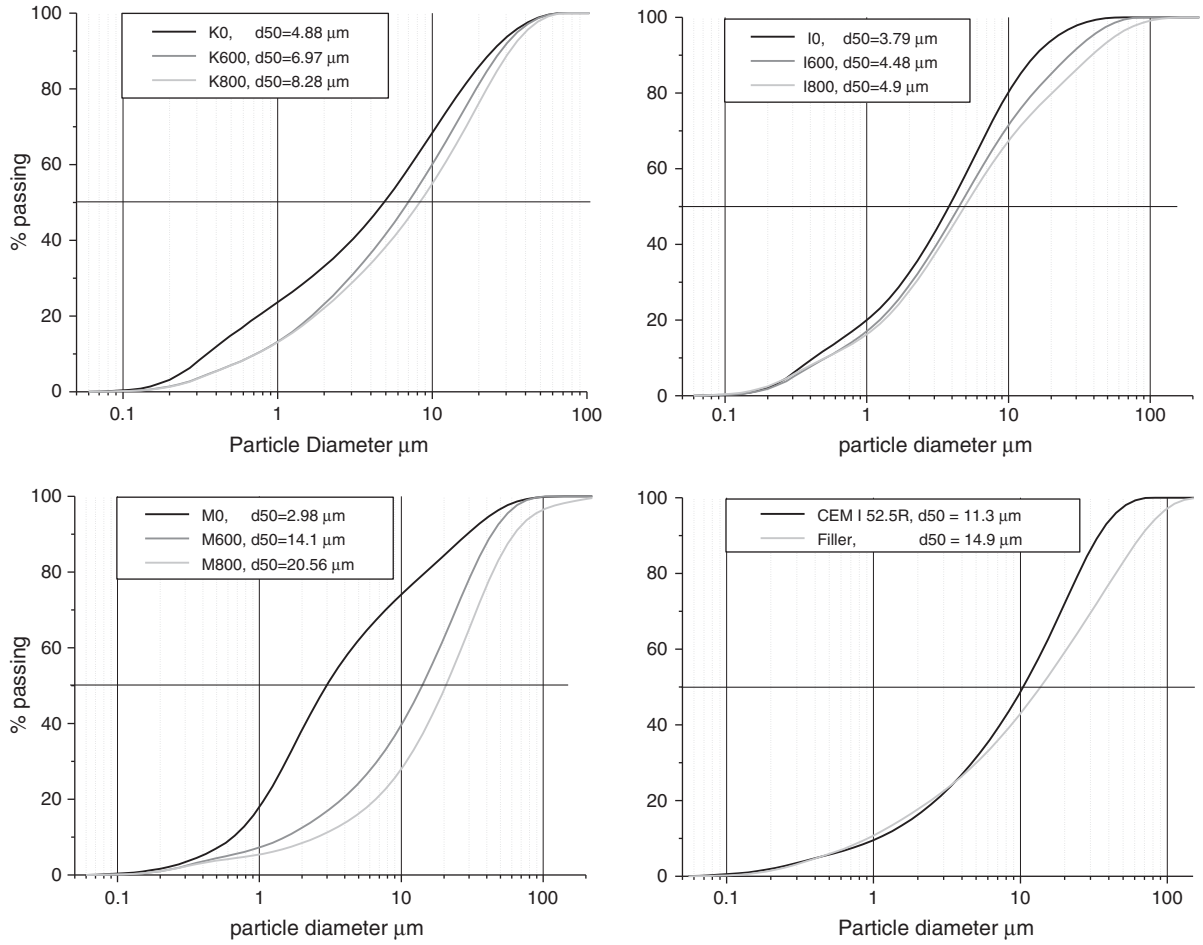

Fig. 6. Particle size distribution of standard clay minerals and their calcined products.

Table 3
Effect of calcinations on different physical properties of the clay minerals.

Method	BET	PSD	He-Picnometer	NMR	XRD
Parameter	Specific Surface [m^2/gr]	Median Diameter d50 [mm]	Bulk Density [gr/cm^3]	Al Coordination	Crystallinity
Kaolinite ref.	26.1512	4.88	2.67	$Al^{[VI]}$	High
Kaolinite 600 °C	24.6978	6.97	2.55	$Al^{[IV]}$, $Al^{[V]}$, and $Al^{[VI]}$	Low
Kaolinite 800 °C	24.1283	8.28	2.65	$Al^{[VI]}$, $Al^{[V]}$, and $Al^{[IV]}$	Low
Illite ref.	21.3277	3.79	2.80	$Al^{[VI]}$ and $Al^{[IV]}$	High
Illite 600 °C	18.4316	4.48	2.69	$Al^{[VI]}$ and $Al^{[IV]}$	High
Illite 800 °C	13.3214	4.9	2.71	$Al^{[IV]}$	High
Montm. Ref.	31.0287	2.98	2.42	$Al^{[VI]}$ and $Al^{[IV]}$	High
Montm. 600 °C	21.386	14.1	2.70	$Al^{[VI]}$ and $Al^{[IV]}$	Medium
Montm. 800 °C	9.7221	20.56	2.58	$Al^{[IV]}$	Medium

clay minerals belonging to the 2:1 layer type. The thermal treatment induces a clear transition from $Al^{[VI]}$ to $Al^{[IV]}$, which occurs at lower temperatures for illite than for montmorillonite. As OH groups in a clayey structure are originally bound to aluminium, this phenomenon corresponds very well with the dehydroxylation observed with DTG. For illite, the loss of hydroxyls is such that in XRD little change in the

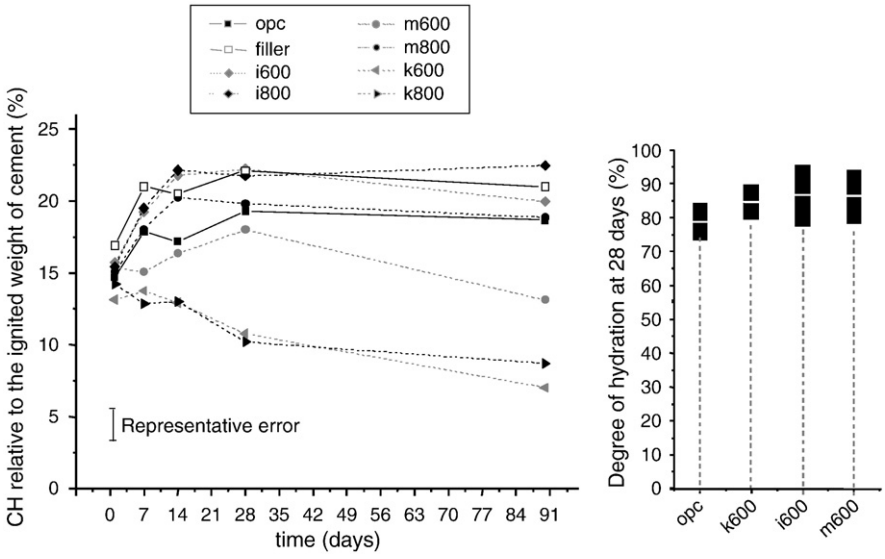

Fig. 7. Calcium hydroxide content (left) and the degree of hydration at 28 days (right).

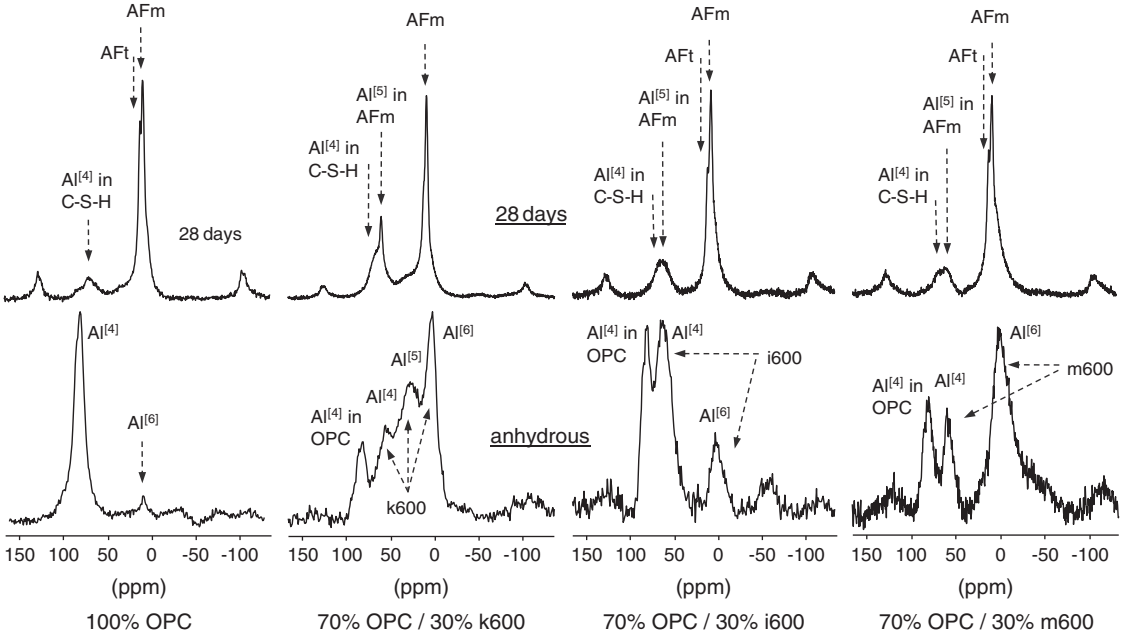

Fig. 8. ^{27}Al NMR spectra of anhydrous blends and pastes at 28 days.

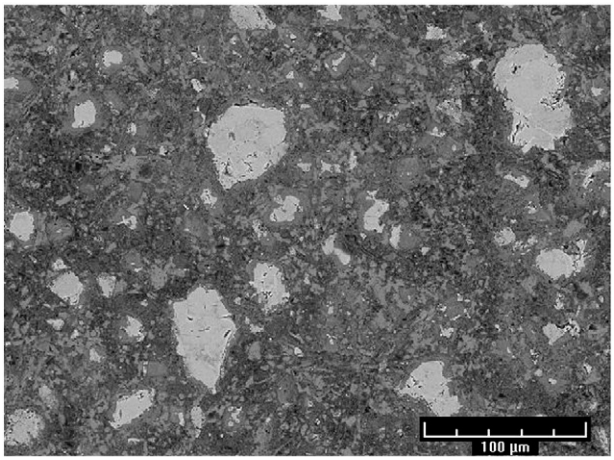

Fig. 9. Microstructure of OPC paste at 28 days (30 °C).

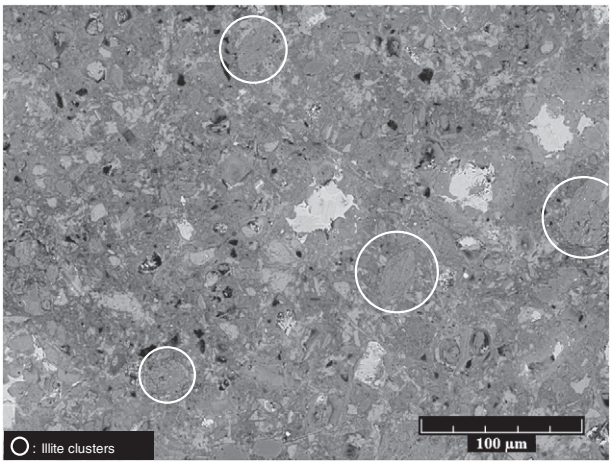

Fig. 11. Microstructure of i600 paste at 28 days (30 °C).

001 spacing of the crystal could be detected (small decrease of the 002, 004, and 0010 peak heights), whereas a reordering in the 110 directions could be observed (increase of the 110 peak). For montmorillonite, dehydroxylation induces a more pronounced decrease of the 001 spacing and almost no reordering in other crystal directions. The fact that the amount of hydroxyls present in the illite and montmorillonite structures is less than for kaolinite could explain the small effect of dehydroxylation on the XRD crystallinity. Thus, kaolinite exhibits a totally different decomposition process that leads to the disordering of the crystal structure, whereas illite and montmorillonite seem to lose their hydroxyls without much change in the crystallographic arrangement of the other atoms.

To gain more knowledge on the changes of the physical properties due to thermal treatment, specific surface, particle size distribution and bulk density were measured. The results are presented in Fig. 6 and Table 3. The increase in median diameter with temperature confirms that thermal treatment tends to agglomerate particles together. This effect is more or less pronounced, depending on the nature of the clay. Agglomeration was found to be the highest for montmorillonite, followed by illite and kaolinite.

3.2. Pozzolanic activity of calcined clay minerals on pastes

Fig. 7 shows the evolution of calcium hydroxide over time for the different cement/calcined clay pastes, together with the degree of hydration of the clinker component at 28 days. Systems incorporating mineral admixtures enhance the hydration of the cement, as values of degree of hydration are centered at 85%, compared to 80%, for the control. This indicates that any substituting material, independent of its pozzolanic properties, induces a filler effect. This is confirmed by the fact that the CH amount, relative to clinker content, for the filler system is at all times higher than the control. Systems incorporating calcined illite have a similar behavior to the filler system, indicating no chemical interaction with cement for this type of calcined clay. However, montmorillonite calcined at 600 °C seems to be effective in consuming calcium hydroxide. The difference between the m600_1 and the m800_1 systems indicates that the reactivity of calcined montmorillonite is more sensitive to the activation temperature than the other clay types. This may be related to the large drop in surface area observed between the samples treated at 600 and 800 °C (Table 3). The calcined kaolinite systems show the most significant pozzolanic activity, with levels of CH being inferior to the reference from early ages. This result shows the reactivity potential of kaolinites over other standard clay minerals commonly found in the earth's crust.

The results of ^{27}Al NMR for the anhydrous mixes and hydrated pastes at 28 days are presented in Fig. 8. The contribution of the calcined clay to the overall signal can be clearly identified in the anhydrous mixes (the small signal for $Al^{[6]}$ in the anhydrous cement can probably be attributed to slight prehydration). The spectra of the hydrated pastes at 28 days reveal the presence of 4 main peaks around 9, 11, 60 and 70 ppm. The first two peaks are assigned to $Al^{[6]}$ in an AFm-type phase and to $Al^{[6]}$ in an AFt-type phase, respectively.

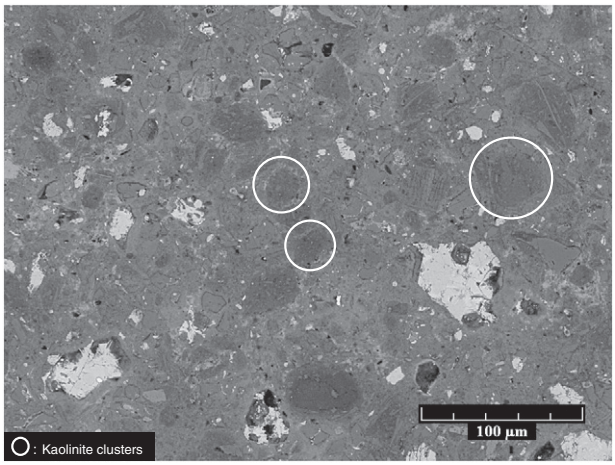

Fig. 10. Microstructure of k600 paste at 28 days (30 °C).

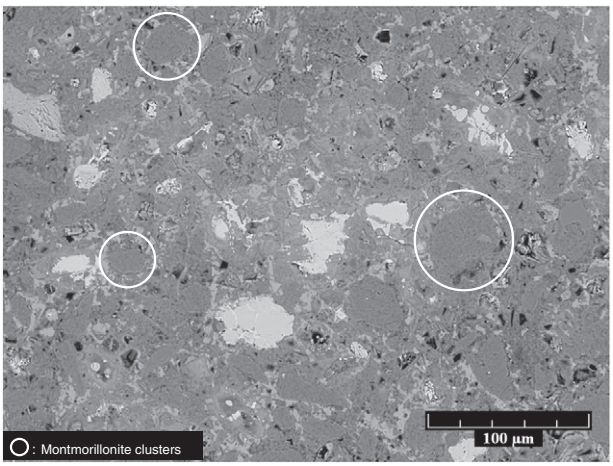

Fig. 12. Microstructure of m600 paste at 28 days (30 °C).

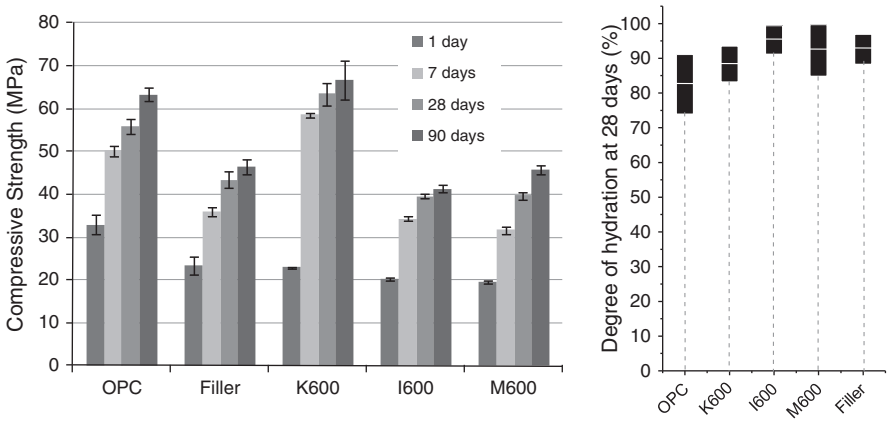

Fig. 13. Compressive strength and degree of hydration at 28 days of calcined-clay-cement mortars.

Following Love et al. [24], while the peak at 70 ppm is assigned to $Al^{[4]}$ in C–S–H, the overlapping peak at 60 ppm is assigned to tetrahedral Al in an aluminosilicate anion in the interlayer of strätlingite (C_2ASH_8), an AFm-type phase. This peak was not detected in the control paste, showing that it is a phase that developed due to the presence of calcined clay in the system. The strong indication of strätlingite in paste k600 could explain the reduced intensity of AFt phases (11 ppm), as one probably develops at the expense of the other. EDS microanalysis indicated some areas with compositions consistent with stratlingite. Due to the fine intermixing of phases, it is not possible to conclude if the stratlingite phase contains other elements (such as sulfate) in a solid solution. Also, according to Faucon et al. [25] and Andersen et al. [26], a minor peak at around 30 ppm could be assigned to $Al^{[5]}$, substituting for Ca in the interlayer of C–S–H. Although this signal can be seen for the hydrated paste k600, it might well be a contribution from $Al^{[5]}$ in calcined kaolinite.

The ^{27}Al NMR results for the reactive clay blends indicate the formation of AFm phases such as strätlingite. This could be due to the fact that more aluminium is provided to the system when calcined clay minerals dissolve in the alkaline environment of the cement paste. In other words, the pozzolanic potential of kaolinite over the other structures could be explained by the fact that its structure has a higher content of hydroxyl groups. As many of these are located at the edge of the structural layer, these groups increase the potential for the creation of disorder by dehydroxilation during thermal treatment. Favoring the dissolution and reaction of aluminium ions with calcium ions provided by the cement.

BSE images of the pastes at 28 days are shown in Figs. 9–12. The pure portland paste exhibits an even distribution of calcium hydroxide crystals over the microstructure. The cement grains are surrounded by a clear layer of "inner" C–S–H hydrate. Several Hadley grains can be identified at the top left area of the image. Dark zones indicate zones of lower density of hydrates and increased quantity of small pores. This coarse porosity is not observed for sample k600, which shows a very homogeneous and dense microstructure. The layer of hydration products around the anhydrous cement grain is less pronounced. This may be due to the presence of calcined clay providing surfaces for the hydrates to nucleate and grow away from the cement grains. Agglomerates of calcined kaolin particles can be easily recognized by their gray level, which is lower than that of CH and even C–S–H. This is due to their low calcium and high alumina content. Although TGA showed that CH is still present in this system at 28 days, CH clusters are not visible in the microstructure, suggesting that CH is more finely divided and part of it reacted with the pozzolan to form AFm and C–S–H phases. Direct evidence of pozzolanic activity is almost impossible to detect in the cement microstructure. First because the most reactive grains are the smaller ones that are difficult to see even at high magnification, and second because the C–S–H they

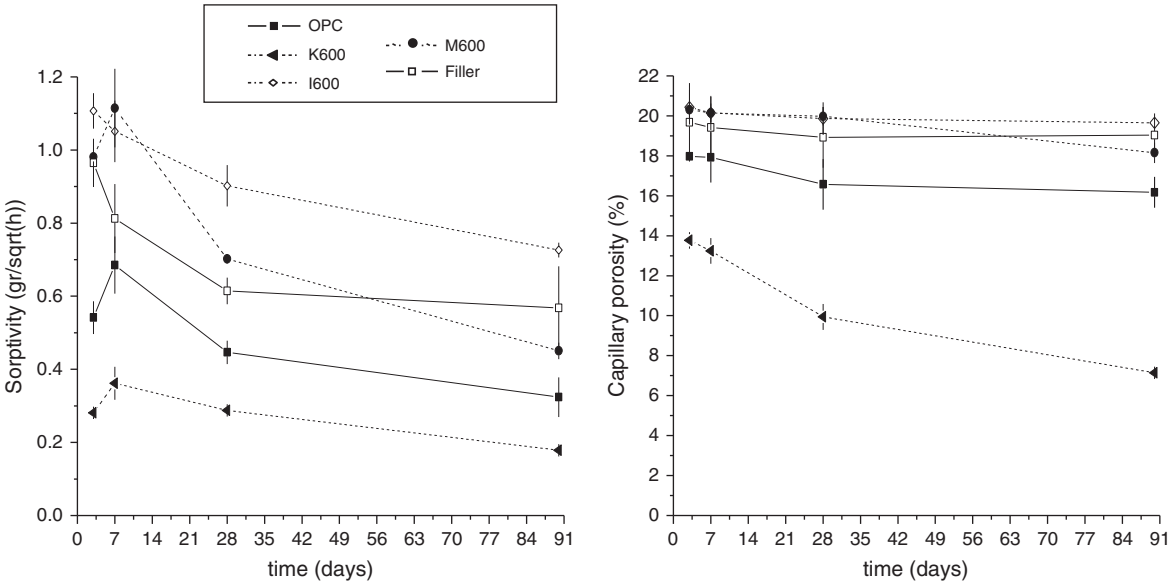

Fig. 14. Sorptivity (left) and capillary porosity (right) of calcined-clay-cement mortars.

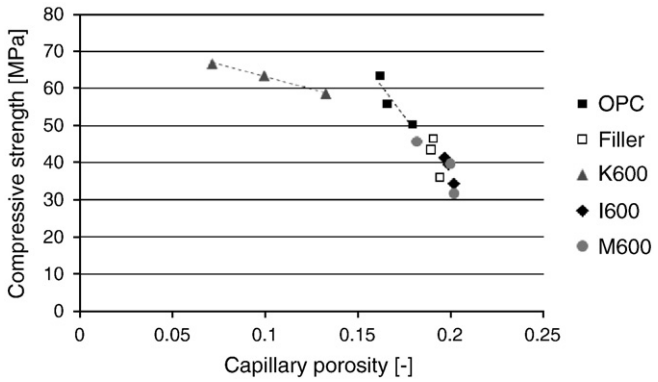

Fig. 15. Correlation of compressive strength with capillary porosity.

form is finely intermixed with the hydrates of the cement and has similar chemical compositions. The microstructure of systems i600 and m600 could be described as very similar to that of OPC, with the difference that calcined clay particles can be observed. Due to differences in composition these particles are more difficult to identify, particularly in the case of calcined illite, which has a gray level similar to that of C–S–H.

3.3. Mechanical properties of calcined-clay–cement mortars

The compressive strength and the degree of hydration for cement in mortars incorporating standard calcined clay are presented in Fig. 13. To assess the contribution of the calcined clay to strength, it is more relevant to compare the blended systems with the blends with filler. The lower strength observed for systems i600, m600 and filler is partly compensated by the higher degree of hydration of the clinker component. This result is coherent with that of the portlandite evolution in the pastes, indicating that illite behaves like an inert filler and montmorillonite exhibits little pozzolanic activity. Note that the late reaction of calcined montmorillonite seen by TGA in pastes does not seem to play much role in the development of the compressive strength between 28 and 90 days, although it is noticeable. The differences in strengths observed between theses low strength mixes might be due to the difference in the physical properties of the substituting materials (see Fig. 6 and Table 3). However, no clear correlation could be made as the particle size distribution of the filler is located between that of illite and montmorillonite, and its specific surface is considerably lower.

The substitution of cement by calcined kaolinite resulted in a considerable increase in strength from 7 days compared to the control mortar. This increase is explained by the pozzolanic character of the calcined clay that combines CH to form additional C–S–H, filling more space and thus increasing the mechanical properties.

In order to explore parameters that might influence the durability of the different systems, the results for sorptivity and capillary porosity (from the final water uptake in the sorptivity tests) are presented in Fig. 14. Nonreactive pozzolans show a poor performance in these tests, with values above those of the inert filler. The system incorporating calcined montmorillonite shows, however, a considerable decrease in sorptivity between 28 and 90 days, which is consistent with the late pozzolanic activity. One the other hand, the system k600 shows much reduced values of sorptivity from early ages, suggesting that additional hydration products were formed through the pozzolanic reaction that resulted in a densification of the microstructure. This system also shows a reduction of the capillary porosity compared to cement. The generally accepted idea that compressive strength is highly dependent on porosity is confirmed in Fig. 15 as the capillary porosity is inversely proportional to the strength for all studied systems.

4. Conclusion

Kaolinite was shown to have the highest potential for activation. This is considered to be due to its higher content of hydroxyl groups and their location in the crystal structure of the clay, which favors more disorder and exposure of Al[5] groups at the surface of the material during the dehydroxilation process. Illite and montmorillonite seem to conserve the order of their structural layers, even after complete dehydroxylation; furthermore, Al groups are trapped between silicate tetrahedral so they are less able to react. This may explain the difficulty of the alkaline medium produced by the hydrating cement to break down the silica or the alumina–silica networks of these clay types.

^{27}Al NMR was found to be a very useful tool for evaluating the state of disorder of the clay minerals. The pozzolanic activity was closely related to the appearance of 5-coordinated aluminium. The monitoring of the calcium hydroxide content gives a good indication of the pozzolanic character of a system compared to the reference cement paste. Again, the system containing calcined kaolinite was the most reactive, followed by calcined montmorillonite, which showed some reactivity at later ages, and calcined illite, which behaved like an inert filler.

The activation temperature did not influence significantly the pozzolanic properties of the calcined clay minerals, except for calcined montmorillonite, whose particle size distribution and specific surface was strongly affected by the increase in calcination temperature. It would be interesting to study this material in a pure state, as the companion minerals it contains could have acted as a flux, leading to sintering at comparatively low temperatures.

^{27}Al NMR on pastes indicated that C–S–H is enriched in Al, which is available due to the dissolution of the pozzolans. This technique also indicated the presence of strätlingite in the calcined-kaolinite–cement system.

The similarities of the 28-day microstructures between systems with calcined illite or calcined montmorillonite with the reference cement paste tend to indicate that these additions have a low activity and do not much influence the microstructural development. However, the microstructure of the calcined-kaolinite–cement system showed different features: a dense microstructure, the absence of visible calcium hydroxide clusters and no hydration rings around cement grains. This suggests that there has been a strong chemical interaction between the pozzolan and the cement from early ages.

The study on mortars confirmed that the pozzolanic activity of the calcined kaolinite can enhance the mechanical properties of cement blends, surpassing that of the 100% cement reference paste already at 7 days. The other blends show mechanical properties similar to the blend with inert filler.

Acknowledgements

The authors thank Dr. Emmanuel Gallucci and Dr. Gwen Le Saout for their assistance in SEM and ^{27}Al NMR, respectively. Dr. Steve Feldman is also acknowledged for bringing his expertise in clay mineralogy and XRD. The research reported in this paper was supported by the Swiss National Science Foundation.

References

[1] B.B. Sabir, S. Wild, J. Bai, Metakaolin and calcined clays as pozzolans for concrete: a review, Cement and Concrete Composites 23 (2001) 441.
[2] S. Wild, J.M. Khatib, Portlandite consumption in metakaolin cement pastes and mortars, Cement and Concrete Research 27 (1997) 137.
[3] M. Singh, M. Garg, Reactive pozzolana from Indian clays–Their use in cement mortars, Cement and Concrete Research 36 (2006) 1903.
[4] M.H. Zhang, V.M. Malhotra, Characteristics of a thermally activated aluminosilicate pozzolanic material and its use in concrete, Cement and Concrete Research 25 (1995) 1713.

[5] G.W. Brindley, M. Nakahira, The Kaolinite-Mullite Reaction Series: II, Metakaolin, Journal of the American Ceramics Society 42 (1959) 314.
[6] I.B. Mackenzie KJD, Outstanding problems in the kaolinite-mullite reaction sequenceinvestigated by Si and Al solid state NMR: I Metakaolinite, Journal of the American Ceramics Society 68 (1985) 293.
[7] J. Rocha, J. Klinowski, 29Si and 27Al magic-angle-spinning NMR studies of the thermal transformation of kaolinite, Physics and Chemistry of Minerals 17 (1990) 179.
[8] E. Lippmaa, A. Samoson, M. Magi, High-resolution aluminum-27 NMR of aluminosilicates, Journal of the American Chemical Society 108 (1986) 1730.
[9] Gilson, Penta-coordinated aluminium in zeolites and aluminosilicates, Journal of the Chemical Society, Chemical Communications 2 (1987) 91.
[10] D.L. Carroll, T.F. Kemp, T.J. Bastow, M.E. Smith, Solid-state NMR characterisation of the thermal transformation of a Hungarian white illite, Solid State Nuclear Magnetic Resonance 28 (2005) 31.
[11] I.W.M. Brown, K.J.D. MacKenzie, R.H. Meinhold, The thermal reactions of montmorillonite studied by high-resolution solid-state29Si and27Al NMR, Journal of Materials Science 22 (1987) 3265.
[12] C. He, B. Osbaeck, E. Makovicky, Pozzolanic reactions of six principal clay minerals: Activation, reactivity assessments and technological effects, Cement and Concrete Research 25 (1995) 1691.
[13] J. Ambroise, M. Murat, J. Pera, Hydration reaction and hardening of calcined clays and related minerals V: Extension of the research and general conclusions, Cement and Concrete Research 15 (1985) 261.
[14] A. Shvarzman, K. Kovler, G.S. Grader, G.E. Shter, The effect of dehydroxylation/amorphization degree on pozzolanic activity of kaolinite, Cement and Concrete Research 33 (2003) 405.
[15] E. Badogiannis, G. Kakali, S. Tsivilis, Metakaolin as supplementary cementitious material, Journal of Thermal Analysis and Calorimetry 81 (2005) 457.
[16] http://wardsci.com.
[17] J.K. Mitchell, Fundamentals of Soil Behaviour, 3rd editionJohn Wiley & Sons, Inc, 2005.
[18] Kátia C. Lombardi, Structural and morphological characterization of the PP-0559 kaolinite from the Brazilian Amazon region, Journal of the Brazilian Chemical Society 13 (2) (2002).
[19] R. Grim, Applied Clay Mineralogy, McGraw-Hill, 1962.
[20] B.K. Marsh, R.L. Day, Pozzolanic and cementitious reactions of fly ash in blended cement pastes, Cement and Concrete Research 18 (1988) 301.
[21] K.L. Scrivener, Backscattered electron imaging of cementitious microstructures: understanding and quantification, Cement and Concrete Composites 26 (2004) 935.
[22] N. Todor, Thermal Analysis of Minerals, Abacus Press, 1976.
[23] Q. Liu, D.A. Spears, Q. Liu, MAS NMR study of surface-modified calcined kaolin, Applied Clay Science 19 (2001) 89.
[24] C.A. Love, I.G. Richardson, A.R. Brough, Composition and structure of C—S—H in white Portland cement-20% metakaolin pastes hydrated at 25C, Cement and Concrete Research 37 (2007) 109.
[25] P. Faucon, A. Delagrave, J.C. Petit, C. Richet, J.M. Marchand, H. Zanni, Aluminum incorporation in calcium silicate hydrates (C–S–H) depending on their Ca/Si ratio, The Journal of Physical Chemistry B 103 (1999) 7796.
[26] M.D. Andersen, H.J. Jakobsen, J. Skibsted, Incorporation of aluminum in the calcium silicate hydrate (C–S–H) of hydrated portland cements: A high-field ^{27}Al and ^{29}Si MAS NMR investigation, Inorganic Chemistry 42 (2003) 2280.